

Anisotropic magnetoresistance of 2D Rashba films with in-plane Zeeman field and short-range disorder

Igor Gornyi^{1,2} and Alexander Khaetskii³

¹*Institute for Quantum Materials and Technologies, Karlsruhe Institute of Technology, 76131 Karlsruhe, Germany*

²*Institut für Theorie der Kondensierten Materie, Karlsruhe Institute of Technology, 76131 Karlsruhe, Germany*

³*Department of Physics and Astronomy, Ohio University, Athens, OH, USA*

(Dated: July 7, 2026)

We study the dc conductivity of a continuum two-dimensional Rashba film with an in-plane Zeeman field and delta-correlated scalar disorder. Although the field deforms the two helicity Fermi contours and rotates the spin texture, it does not produce anisotropic magnetoresistance in the leading quasiclassical conductivity. The mechanism is geometric. A density Ward identity fixes the spin-vector part of the Born self-energy to the derivative of the total particle density with respect to the field. This derivative vanishes, because the total area enclosed by the two Rashba-Zeeman sheets is independent of the in-plane field. The Born self-energy is therefore scalar and field independent, and the quasiparticle lifetime stays isotropic. The same area invariance controls transport: once the leading impurity ladder reduces the current vertex to the parabolic velocity, the diagonal intraband Kubo conductivity collapses onto the two-sheet occupied area and is field independent as well. The result settles the short-range-disorder quasiclassical problem: point-like nonmagnetic impurities do not produce AMR in this model. A nonzero AMR requires physics beyond this quasiclassical short-range-disorder mechanism.

I. INTRODUCTION

Anisotropic magnetoresistance (AMR)-the dependence of electrical resistance on the direction of an applied magnetic field or magnetization-is a long-standing phenomenon with both fundamental and technological importance [1]. In low-dimensional conductors with spin-orbit coupling, such as semiconductor and oxide two-dimensional electron gases, an in-plane Zeeman field breaks spin-rotation symmetry, changes the momentum-dependent spin orientation of the electronic states, and deforms the helicity Fermi contours. This makes Rashba systems with an in-plane field a natural minimal setting for discussing AMR without magnetic order. The central question is which microscopic ingredients are sufficient to produce a finite AMR.

The answer in the literature has not been uniform. Raimondi *et al.* [2] studied essentially the same single-band Rashba-Zeeman problem with scalar short-range disorder. Their paper is especially important because it compared a relaxation-time kinetic treatment with a diagrammatic Kubo calculation including impurity vertex corrections. The two approaches did not give the same anisotropy; even the sign changed after the vertex corrections were included. At the same time, Raimondi *et al.* already identified a crucial element of the correct short-range-disorder calculation: in the weak-field metallic regime the impurity ladder strongly cancels the anomalous Rashba velocity, so that the dressed retarded-advanced current vertex is close to the parabolic one. Their remaining finite numerical AMR is therefore not a consequence of simply omitting vertex corrections. It appears in a broader finite-broadening/high-field calculation, with the strongest structure near the spin-polarization scale, where the Zeeman energy is of order the Fermi energy.

Related work reached different conclusions from different angles. Inoue *et al.* [3] showed, for the anomalous Hall response of a spin-polarized Rashba model, that the intrinsic contribution is removed by vertex corrections unless the quasiparticle lifetime is spin dependent. Kato *et al.* [4] formulated the analogous cancellation criterion for intrinsic AMR. Trushin *et al.* [5] studied carriers with Rashba and Dresselhaus couplings scattered by polarized magnetic impurities, thereby addressing a different magnetic-disorder mechanism. Wang and Pang [6] performed a numerical study that made a sharp distinction between point-like and remote nonmagnetic impurities: the AMR vanished for delta-function disorder but became finite for long-range disorder. Wang later extended this analysis to combined Rashba-Dresselhaus systems and again emphasized that, for short-range spin-independent disorder, AMR vanishes when both helicity bands are occupied, while this cancellation no longer applies in the single-band regime [7]. The long-range and nonparabolic mechanisms were explored further in Ref. [8]. Vaz *et al.* [9] used bilinear magnetoresistance to extract an effective Rashba parameter in an oxide two-dimensional electron gas. Their microscopic theory is directly relevant here because it also uses a local scalar impurity potential, a Born self-energy, and impurity vertex corrections, but it contains a field-dependent relaxation-time structure.

Together, these results leave a concrete puzzle. In the point-like nonmagnetic-disorder model, some calculations find no AMR, whereas other short-range-disorder treatments contain a finite anisotropy or a field-dependent scalar lifetime. Moreover, the numerical works that find zero AMR for delta disorder usually address angular anisotropy under rotation of the magnetization, not the stronger question whether the diagonal quasiclassical conductivity itself is independent of the field magnitude.

This difference cannot be dismissed as a comparison between unrelated physical systems: the Rashba–Zeeman Hamiltonian, scalar disorder, and impurity ladder are common ingredients. The present paper resolves this problem for the leading diagonal two-sheet quasiclassical sector. In this sector, the scalar Born lifetime is not an independent angle-dependent input, and the leading diagonal conductivity is not a generic functional of the separately distorted contours. Both quantities are fixed by the same geometric identity. As a result, the quasiclassical conductivity does not depend on the in-plane magnetic field.

The first part of the argument concerns the Born self-energy. For short-range scalar disorder, the self-energy is the full momentum-integrated on-shell spectral matrix. Its spin-vector part is related to the derivative of the total density with respect to the in-plane Zeeman field. This identity is the Zeeman analogue of the thermodynamic logic behind Středa’s formula [10]: a Fermi-sea derivative fixes a Fermi-surface response. In the continuum parabolic Rashba model with both helicity sheets included, the total occupied area is unchanged by the displacement of the Rashba degeneracy point. Therefore, the spin-vector part of the Born broadening vanishes and the projected quasiparticle lifetime is the field-independent scalar lifetime τ_0 . The perturbative calculation in Sec. S2 of the Supplemental Material shows explicitly how an apparent anisotropic lifetime is removed once the density-of-states factor and the spin projector are evaluated on the same helicity Fermi sheet.

The second part of the argument concerns the current vertex. A point-like impurity potential does not mean that the transport vertex is bare in a spin–orbit-coupled band. The spinor overlap makes the projected transport kernel nontrivial. The impurity ladder cancels the anomalous Rashba part of the bare velocity and leaves the parabolic current vertex. This cancellation is not a weak-spin-orbit expansion: it follows from derivatives of the same occupied-area identity that controls the Born self-energy. With this dressed vertex, the diagonal intraband Kubo integral becomes a geometric contour integral. The azimuthal part of the band velocity converts by integration by parts into the area enclosed by the Fermi contour, and the sum over the two helicity sheets is the field-independent total area. Thus, the Fermi-contour deformation, the spin-texture rotation, the scalar Born lifetime, and the impurity ladder together give no AMR for point-like scalar disorder; in fact, within this diagonal quasiclassical sector, they give no field dependence of the longitudinal conductivity.

This result should be read as a settlement of the leading quasiclassical short-range-disorder mechanism. It agrees with the vanishing delta-disorder AMR found by Wang and Pang and identifies why finite AMR from remote impurities is a different mechanism. It also clarifies the relation to Raimondi *et al.*: their ladder cancellation of the anomalous Rashba velocity is confirmed and strengthened, while their finite numerical AMR belongs

to a broader finite-broadening/high-field calculation and should not be interpreted as the protected diagonal two-sheet quasiclassical contribution. More generally, short-range-disorder calculations based on a field-dependent scalar relaxation time are incorrect for the continuum two-sheet model: they miss the Ward-identity cancellation of the spin-vector spectral weight, or equivalently mix quantities that must be evaluated on the same helicity Fermi sheet.

The paper is organized as follows. Section II introduces the Rashba–Zeeman Hamiltonian and the two-sheet regime. Section III derives the Born self-energy and the Ward identity for the scalar lifetime. Section IV evaluates the diagonal intraband Kubo conductivity and reduces it to the total occupied area. Section V compares the result with previous work and identifies which short-range-disorder claims are consistent with the present Ward-identity calculation. Appendix S3 proves the area identity, and Appendix B gives the impurity-ladder vertex. The Supplemental Material (SM) [11] gives the projected Dyson derivation, the perturbative weak-field check of the lifetime cancellation, and an alternative shifted-coordinate proof of the area identity.

II. THE SYSTEM

A. Hamiltonian

The Hamiltonian of the problem and the velocity operator are:

$$\hat{H}(\mathbf{p}) = \frac{\mathbf{p}^2}{2m} \hat{I} + \alpha \hat{\boldsymbol{\sigma}} \cdot \mathbf{p} + \mathbf{B} \cdot \hat{\boldsymbol{\sigma}}; \quad (1)$$

$$\hat{v}(\mathbf{p}) = \frac{\partial \hat{H}}{\partial \mathbf{p}} = \frac{\mathbf{p}}{m} \hat{I} + \alpha \hat{\boldsymbol{\sigma}}. \quad (2)$$

Here, \mathbf{p} is the two-dimensional electron momentum, α is the Rashba spin-orbit coupling, and $\hat{\boldsymbol{\sigma}}$ are the Pauli matrices. Bold symbols denote two-dimensional vectors. The orbital coupling to the magnetic field is absent; only the in-plane Zeeman term is retained. We write the Zeeman coupling entering the Hamiltonian as an energy-valued vector

$$\mathbf{B} = B \mathbf{e}_B, \quad \mathbf{e}_B = (\cos \phi_B, \sin \phi_B), \quad B = |\mathbf{B}|. \quad (3)$$

The sign of the microscopic Zeeman coupling has been absorbed into \mathbf{B} . If \mathcal{B} denotes the magnitude of the physical magnetic field, then $B = g\mu_B \mathcal{B}/2$ up to this sign convention. In what follows, we use units with $\hbar = 1$.

The eigenvalues of the Hamiltonian are

$$\begin{aligned} \epsilon_{\pm}(\mathbf{p}) &= \frac{p^2}{2m} \pm |\alpha \mathbf{p} + \mathbf{B}| \\ &= \frac{p^2}{2m} \pm \sqrt{(\alpha p)^2 + B^2 + 2\alpha p B \cos \theta}, \end{aligned} \quad (4)$$

where θ is the angle between \mathbf{p} and \mathbf{B} . The band velocities obtained from the dispersion are

$$\mathbf{v}_{\pm} = \frac{\mathbf{p}}{m} \pm \alpha \nu_{\mathbf{p}}, \quad \nu_{\mathbf{p}}(\mathbf{B}) = \frac{\alpha \mathbf{p} + \mathbf{B}}{|\alpha \mathbf{p} + \mathbf{B}|}, \quad (5)$$

where $\nu_{\mathbf{p}}$ is the unit vector in the direction of the local Rashba-Zeeman field. The two branches of the energy spectrum correspond to positive and negative eigenvalues of the chirality operator

$$\hat{\nu}(\mathbf{p}) = \nu_{\mathbf{p}} \cdot \hat{\sigma}. \quad (6)$$

The projectors onto these branches are

$$\hat{\Omega}_{\pm}(\mathbf{p}) = \frac{1 \pm \hat{\nu}(\mathbf{p})}{2}. \quad (7)$$

We consider a short-ranged impurity potential $V_{\text{imp}} = \sum_i U \delta(\mathbf{r} - \mathbf{R}_i)$; in the absence of Zeeman field the Born scattering rate is

$$\frac{1}{\tau_0} = 2\pi n_{\text{imp}} |U|^2 \nu_0 = n_{\text{imp}} |U|^2 m, \quad (8)$$

where n_{imp} is the 2D impurity concentration and $\nu_0 = m/2\pi$ is the density of states per spin in two dimensions. Throughout the paper we work in the clean two-sheet metallic regime $E_F \tau_0 \gg 1$ and $\alpha p_F \tau_0 \gg 1$, in which the two helicity bands are resolved on the scale of the disorder broadening (the narrow Lifshitz window $|\gamma - 1| \lesssim \epsilon_{\tau}$ introduced below is excluded by this assumption).

B. Spectrum

The local band splitting is

$$\Delta(\mathbf{p}) = 2|\alpha \mathbf{p} + \mathbf{B}|.$$

It vanishes at the Rashba-Zeeman degeneracy point

$$\mathbf{p}_* = -\frac{\mathbf{B}}{\alpha}. \quad (9)$$

This point exists for every value of the in-plane field. What changes with the field is whether the degeneracy point lies on the Fermi surface. Its energy is purely kinetic,

$$E_* = \frac{p_*^2}{2m} = \frac{B^2}{2m\alpha^2}. \quad (10)$$

Then we obtain

$$E_* = \gamma^2 E_F, \quad E_F = \frac{p_F^2}{2m}, \quad \gamma = \frac{B}{\alpha p_F}. \quad (11)$$

Thus, the degeneracy point lies below the Fermi energy for $\gamma < 1$, on the Fermi surface for $\gamma = 1$, and above the Fermi energy for $\gamma > 1$. The point $\gamma = 1$ is the Lifshitz crossing relevant for the on-shell quasiparticle problem:

the degeneracy point itself does not disappear for $\gamma > 1$, but it is then off shell.

We use $p_F = \sqrt{2mE_F}$ as the reference Fermi momentum of the parabolic band at the chosen chemical potential. Near the antiparallel direction we write $\theta = \phi - \phi_B = \pi + \eta$, $|\eta| \ll 1$. Therefore the on-shell splitting behaves as

$$\Delta(\eta) \simeq 2\alpha p_F \sqrt{(\gamma - 1)^2 + \gamma \eta^2}. \quad (12)$$

The minimum splitting on the Fermi surface is $\Delta_{\text{min}} \simeq 2\alpha p_F |\gamma - 1|$. It vanishes only at $\gamma = 1$.

We will work in the two-sheet regime throughout the main calculation. By this we mean that both helicity branches cross the chemical potential for every direction in momentum space, so that each branch is described by a single positive outer Fermi radius $\mathbf{p}_s(\phi) = p_s(\phi) \mathbf{e}_{\phi}$, $s = \pm$. In particular, the $s = +$ sheet is present only when $\mu = E_F > B$.

For $\gamma < 1$ the Fermi contours enclose the degeneracy point, and the spin texture winds once around it. For $\gamma > 1$ the degeneracy point lies outside the Fermi contours at energy E_F , and the on-shell spin texture has no such winding. This change of the Fermi-surface geometry relative to the Rashba degeneracy is the Lifshitz crossing referred to below.

The diagonal helicity projection is controlled when the local splitting is large compared with the disorder broadening. Near $\theta = \pi$, this gives the disorder-broadened Lifshitz window

$$|\gamma - 1| \lesssim \epsilon_{\tau}, \quad \epsilon_{\tau} = \frac{1}{2\alpha p_F \tau_0}. \quad (13)$$

III. DYSON EQUATION AND SCALAR BORN LIFETIME

We now derive the scalar lifetime that enters the diagonal conductivity calculation. The important point is that the short-range Born self-energy is momentum independent but remains a matrix in spin space. When this matrix is projected onto the local helicity eigenstates, an angle-dependent lifetime is possible in a generic spin-orbit model. In the present continuum Rashba model, however, the spin-vector part of the on-shell Born self-energy vanishes by a Ward identity. The resulting scalar lifetime is isotropic.

A. Born self-energy and projected scattering rate

For a short-range scalar impurity potential, $\langle U(\mathbf{r})U(\mathbf{r}') \rangle = n_{\text{imp}} |U|^2 \delta(\mathbf{r} - \mathbf{r}')$, the Born self-energy is

$$\hat{\Sigma}^R(\epsilon) = n_{\text{imp}} |U|^2 \int \frac{d^2 p}{(2\pi)^2} \hat{G}^{R,0}(\epsilon, \mathbf{p}). \quad (14)$$

Here the clean retarded Green's function is

$$\hat{G}^{R,0}(\epsilon, \mathbf{p}) = \frac{\hat{\Omega}_+(\mathbf{p})}{\epsilon - \epsilon_+(\mathbf{p}) + i0^+} + \frac{\hat{\Omega}_-(\mathbf{p})}{\epsilon - \epsilon_-(\mathbf{p}) + i0^+}. \quad (15)$$

Evaluating the radial integral on shell at $\epsilon = \mu$, one obtains

$$-\text{Im} \hat{\Sigma}^R(\mu) = \pi n_{\text{imp}} |U|^2 \sum_{s=\pm} \int \frac{d^2p}{(2\pi)^2} \delta(\mu - \epsilon_s(\mathbf{p})) \hat{\Omega}_s(\mathbf{p}), \quad (16)$$

where the projector operator is given by Eq. (7), and on the Fermi contour of branch s we write (with $\mathbf{p}_s(\phi) = p_s(\phi) \mathbf{e}_\phi$, $\mathbf{e}_\phi = (\cos \phi, \sin \phi)$, and $\mathbf{e}_\theta = (-\sin \phi, \cos \phi)$)

$$\boldsymbol{\nu}^{(s)}(\phi) \equiv \boldsymbol{\nu}_{\mathbf{p}} \Big|_{\mathbf{p}=\mathbf{p}_s(\phi)} = \frac{\alpha p_s(\phi) \mathbf{e}_\phi + \mathbf{B}}{|\alpha p_s(\phi) \mathbf{e}_\phi + \mathbf{B}|}. \quad (17)$$

Projecting Eq. (16) onto a local helicity state $|s, \phi\rangle$ gives the branch-resolved Golden-Rule rate (see Sec. S1 of SM for details)

$$\begin{aligned} \frac{1}{\tau_s(\phi)} &= 2\pi n_{\text{imp}} |U|^2 \\ &\times \sum_{s'=\pm} \int_0^{2\pi} \frac{d\phi'}{2\pi} \rho_{s'}(\phi') \frac{1 + s s' \boldsymbol{\nu}^{(s)}(\phi) \cdot \boldsymbol{\nu}^{(s')}(\phi')}{2}. \end{aligned} \quad (18)$$

Here,

$$\rho_s(\phi) = \frac{p_s(\phi)}{2\pi |v_{s,\parallel}(\phi)|}, \quad v_{s,\parallel}(\phi) = \left. \frac{\partial \epsilon_s(p, \phi)}{\partial p} \right|_{p=p_s(\phi)} \quad (19)$$

are the angular density of states and the radial velocity on sheet s . The spin texture must be evaluated on the same sheet. The correction to the spin texture caused by the branch-dependent displacement of the Fermi sheet is of the same order as the correction to the angular density of states and cancels the apparent anisotropy. The detailed projection algebra is given in Sec. S1 of the SM.

B. Ward identity behind the isotropic lifetime

The cancellation of the anisotropic scalar lifetime is not an accident of the low-order expansion. It follows from a Ward identity that relates the spin-vector part of the Born broadening to the derivative of the total particle density with respect to the in-plane Zeeman field.

We decompose the on-shell Born broadening as

$$-\text{Im} \hat{\Sigma}^R = \Gamma_0 \hat{I} + \boldsymbol{\Gamma} \cdot \hat{\boldsymbol{\sigma}}. \quad (20)$$

The scalar part is proportional to the total on-shell density of states, while the spin-vector part is

$$\boldsymbol{\Gamma} = \frac{\pi n_{\text{imp}} |U|^2}{2} \sum_s s \int \frac{d^2p}{(2\pi)^2} \delta(\mu - \epsilon_s) \boldsymbol{\nu}_{\mathbf{p}}. \quad (21)$$

A quasiparticle on branch s and angle ϕ sees the projection of this total matrix,

$$\frac{1}{2\tau_s(\phi)} = \Gamma_0 + s \boldsymbol{\Gamma} \cdot \boldsymbol{\nu}^{(s)}(\phi). \quad (22)$$

For the Rashba-Zeeman spectrum

$$\epsilon_s(\mathbf{p}) = \frac{p^2}{2m} + s |\alpha \mathbf{p} + \mathbf{B}|,$$

one has $\partial \epsilon_s / \partial \mathbf{B} = s \boldsymbol{\nu}_{\mathbf{p}}$. Therefore the spin-vector spectral weight in Eq. (21) can be written as

$$\begin{aligned} \mathbf{M}_{\text{FS}}(\mu, \mathbf{B}) &\equiv \sum_s s \int \frac{d^2p}{(2\pi)^2} \delta(\mu - \epsilon_s) \boldsymbol{\nu}_{\mathbf{p}} \\ &= \sum_s \int \frac{d^2p}{(2\pi)^2} \delta(\mu - \epsilon_s) \frac{\partial \epsilon_s}{\partial \mathbf{B}}. \end{aligned} \quad (23)$$

On the other hand, the total density is

$$n(\mu, \mathbf{B}) = \sum_s \int \frac{d^2p}{(2\pi)^2} \Theta(\mu - \epsilon_s(\mathbf{p})). \quad (24)$$

Differentiating it with respect to \mathbf{B} gives

$$\mathbf{M}_{\text{FS}}(\mu, \mathbf{B}) = -\frac{\partial n(\mu, \mathbf{B})}{\partial \mathbf{B}}. \quad (25)$$

This is the Ward identity behind the cancellation. It is the Zeeman analogue of the thermodynamic logic behind Středa's formula [10]: a derivative of an equilibrium Fermi-sea quantity fixes a Fermi-surface spectral response. In the continuum parabolic model with both helicity sheets included, the total occupied area is independent of the displacement of the Rashba degeneracy point by the in-plane field, $\partial n(\mu, \mathbf{B}) / \partial \mathbf{B} = 0$. The proof is given in Appendix S3. With the standard continuum convention, Eqs. (A18) and (A19) give

$$n(\mu, \mathbf{B}) = n(\mu, 0) = \frac{m\mu}{\pi} + \frac{m^2 \alpha^2}{\pi}. \quad (26)$$

Thus, the spin-vector part of the on-shell Born broadening vanishes:

$$\boldsymbol{\Gamma} = 0, \quad -\text{Im} \hat{\Sigma}^R = \Gamma_0 \hat{I}. \quad (27)$$

The branch-projected scalar lifetime is therefore isotropic and field independent:

$$\frac{1}{\tau_s(\phi)} = 2\Gamma_0 \equiv \frac{1}{\tau_0}. \quad (28)$$

The scalar lifetime result is exact within the continuum two-sheet, on-shell Born model for short-range disorder.

IV. CONDUCTIVITY

A. General framework

We start from the retarded-advanced part of the disorder-averaged Kubo formula,

$$\sigma_{ij} = \left\langle \frac{e^2}{2\pi} \int \frac{d^2\mathbf{p}}{(2\pi)^2} \text{tr} [\hat{v}_i(\mathbf{p}) G^A(\mu, \mathbf{p}) \hat{v}_j(\mathbf{p}) G^R(\mu, \mathbf{p})] \right\rangle. \quad (29)$$

Here, the trace is over spin, $\langle \dots \rangle$ denotes disorder averaging, and μ is the chemical potential. The quasiclassical conductivity considered below in the regime $E_F\tau_0 \gg 1$ is

the leading metallic dc contribution obtained from this $G^A G^R$ bubble after the on-shell projection to the helicity Fermi contours and the corresponding impurity-ladder renormalization of the current vertex.

With the scalar broadening inserted, the diagonal helicity Green's functions used in this section are

$$\hat{G}^{R,A}(\mu, \mathbf{p}) = \sum_{s=\pm} \frac{\hat{\Omega}_s(\mathbf{p})}{\mu - \epsilon_s(\mathbf{p}) \pm i/(2\tau_0)}. \quad (30)$$

Using the leading ladder correction derived in Appendix B, we write $\hat{V}_i^{\text{lead}} = p_i/m$ for the dressed vertex in the diagonal intraband calculation below. Keeping only intraband Kubo pairs, we obtain

$$\sigma_{ij} = \frac{e^2}{2\pi} \int \frac{d^2\mathbf{p}}{(2\pi)^2} \left(\frac{\mathbf{p}}{m} \right)_i \left[\frac{\left(\frac{\mathbf{p}}{m} + \alpha\boldsymbol{\nu}_\mathbf{p} \right)_j}{[\mu - \epsilon_+(\mathbf{p}) - i/2\tau_0][\mu - \epsilon_+(\mathbf{p}) + i/2\tau_0]} + \frac{\left(\frac{\mathbf{p}}{m} - \alpha\boldsymbol{\nu}_\mathbf{p} \right)_j}{[\mu - \epsilon_-(\mathbf{p}) - i/2\tau_0][\mu - \epsilon_-(\mathbf{p}) + i/2\tau_0]} \right]. \quad (31)$$

Here, $\boldsymbol{\nu}_\mathbf{p}$ is defined by Eq. (5).

Integrating over $\xi = \epsilon_s(\mathbf{p}) - \mu$ on each helicity branch, we obtain the Fermi-surface contribution

$$\sigma_{ij} = e^2\tau_0 \int_0^{2\pi} \frac{d\phi}{(2\pi)^2} \left\{ \frac{p(\mathbf{p}/m)_i (\mathbf{p}/m + \alpha\boldsymbol{\nu}_\mathbf{p})_j}{p/m + \alpha\boldsymbol{\nu}_\mathbf{p} \cdot \mathbf{e}_\phi} \Big|_{p=p_+} + \frac{p(\mathbf{p}/m)_i (\mathbf{p}/m - \alpha\boldsymbol{\nu}_\mathbf{p})_j}{p/m - \alpha\boldsymbol{\nu}_\mathbf{p} \cdot \mathbf{e}_\phi} \Big|_{p=p_-} \right\}. \quad (32)$$

Here, $p_\pm(\phi)$ are the solutions of $\epsilon_\pm(p, \phi) = \mu$. All quantities in each term, including $\boldsymbol{\nu}_\mathbf{p}$, are evaluated at the same on-shell momentum $p = p_\pm(\phi)$.

B. Diagonal quasiclassical conductivity

We now evaluate the diagonal intraband contribution to the quasiclassical dc conductivity in the split-band regime where the helicity projection is controlled. On helicity sheet s , let $p_s(\phi)$ be the outer Fermi radius. The band velocity is

$$\mathbf{v}_s(\mathbf{p}) = \nabla_{\mathbf{p}} \epsilon_s(\mathbf{p}) = \frac{\mathbf{p}}{m} + s\alpha\boldsymbol{\nu}_\mathbf{p}. \quad (33)$$

Its radial component $v_{s,\parallel} = \mathbf{v}_s \cdot \mathbf{e}_\phi$ is

$$v_{s,\parallel}(\phi) = \frac{\partial \epsilon_s}{\partial p} \Big|_{p=p_s(\phi)} = \frac{p_s(\phi)}{m} + s\alpha\boldsymbol{\nu}^{(s)}(\phi) \cdot \mathbf{e}_\phi, \quad (34)$$

where $\boldsymbol{\nu}^{(s)}(\phi) = \boldsymbol{\nu}_\mathbf{p}|_{\mathbf{p}=p_s(\phi)\mathbf{e}_\phi}$. Thus, the denominator in the s -branch term of Eq. (32) is precisely the radial velocity $v_{s,\parallel}(\phi)$. Then the s -branch contribution to Eq. (32) can be rewritten as

$$\sigma_{xx}^{(s)} = e^2\tau_0 \int_0^{2\pi} \frac{d\phi}{(2\pi)^2} p_s(\phi) \frac{(\mathbf{p}/m)_x (\mathbf{p}/m + s\alpha\boldsymbol{\nu}_\mathbf{p})_x}{p/m + s\alpha\boldsymbol{\nu}_\mathbf{p} \cdot \mathbf{e}_\phi} \Big|_{\mathbf{p}=p_s(\phi)\mathbf{e}_\phi} = e^2\tau_0 \int_0^{2\pi} \frac{d\phi}{(2\pi)^2} p_s(\phi) \frac{[p_s(\phi) \cos \phi/m] v_{s,x}(\phi)}{v_{s,\parallel}(\phi)}. \quad (35)$$

The Fermi contour is defined by $\epsilon_s[p_s(\phi), \phi] = \mu$. Differentiating this identity with respect to ϕ gives

$$\frac{d}{d\phi} \epsilon_s[p_s(\phi), \phi] = \frac{\partial \epsilon_s}{\partial \phi} \Big|_{p=p_s(\phi)} + v_{s,\parallel} \frac{dp_s}{d\phi} = 0. \quad (36)$$

Therefore, on the Fermi contour, the azimuthal velocity is

$$v_{s,\phi}(\phi) = \mathbf{v}_s \cdot \mathbf{e}_\theta = \frac{1}{p_s(\phi)} \frac{\partial \epsilon_s}{\partial \phi} \Big|_{p=p_s(\phi)} = -\frac{v_{s,\parallel}(\phi)}{p_s(\phi)} \frac{dp_s(\phi)}{d\phi}, \quad (37)$$

and the x -component of the velocity is

$$v_{s,x}(\phi) = v_{s,\parallel}(\phi) \cos \phi - v_{s,\phi}(\phi) \sin \phi = v_{s,\parallel}(\phi) \left[\cos \phi + \frac{\sin \phi}{p_s(\phi)} \frac{dp_s(\phi)}{d\phi} \right]. \quad (38)$$

Using Eq. (38) in Eq. (35), we obtain

$$\sigma_{xx}^{(s)} = \frac{e^2 \tau_0}{m} \int_0^{2\pi} \frac{d\phi}{(2\pi)^2} \left[p_s^2(\phi) \cos^2 \phi + p_s(\phi) \frac{dp_s(\phi)}{d\phi} \sin \phi \cos \phi \right]. \quad (39)$$

The second term is the geometric correction from the azimuthal velocity component: it appears because the band velocity is normal to the distorted Fermi contour rather than purely radial. The second term becomes an area contribution after integration by parts:

$$\int_0^{2\pi} d\phi p_s(\phi) \frac{dp_s(\phi)}{d\phi} \sin \phi \cos \phi = -\frac{1}{2} \int_0^{2\pi} d\phi p_s^2(\phi) \cos 2\phi. \quad (40)$$

Combining this with Eq. (39) gives

$$\sigma_{xx}^{(s)} = \frac{e^2 \tau_0}{2m} \int_0^{2\pi} \frac{d\phi}{(2\pi)^2} p_s^2(\phi). \quad (41)$$

Thus, each branch contributes only through the area enclosed by its Fermi contour. Using the polar-area representation introduced in Eq. (A4), the sum over the two helicity sheets gives

$$\sigma_{xx} = \frac{e^2 \tau_0}{(2\pi)^2} \frac{1}{2m} \int_0^{2\pi} d\phi [p_+^2(\phi) + p_-^2(\phi)] = \frac{e^2 \tau_0}{(2\pi)^2 m} A_{\text{tot}}^{(p)}. \quad (42)$$

Hence, within the scalar-lifetime and leading-vertex diagonal approximation, σ_{xx} is determined only by the total occupied area of the two helicity sheets. Using the density-area relation in Eq. (A19), Eq. (42) takes the Drude form

$$\sigma_{xx}(B) = \frac{e^2 n(\mu, \mathbf{B}) \tau_0}{m}. \quad (43)$$

The area identity proved in Appendix S3 gives $n(\mu, \mathbf{B}) = n(\mu, 0)$, and therefore

$$\sigma_{xx}(B) = \sigma_{xx}(0) = \frac{e^2 \tau_0}{2\pi m} [p_F^2 + 2(m\alpha)^2] \quad (44)$$

is independent of \mathbf{B} . The same contour argument, with x replaced by y , gives $\sigma_{yy}(B) = \sigma_{yy}(0) = \sigma_{xx}(0)$, and hence

$$\sigma_{xx} - \sigma_{yy} = 0. \quad (45)$$

Equations (44) and (45) are the central transport result of the paper. The deformation of the two helicity Fermi contours, the rotation of the spin texture, the scalar Born lifetime, and the leading impurity ladder do not produce AMR for point-like nonmagnetic disorder in the continuum two-sheet quasiclassical model.

V. COMPARISON WITH PREVIOUS RESULTS

The closest comparison is with Raimondi *et al.* [2]. Their model contains the same ingredients that are central here: a single parabolic two-dimensional band, Rashba spin-orbit coupling, an in-plane Zeeman field, scalar short-range disorder, and impurity vertex corrections. Their work is especially useful because it already shows where the problem lies. A relaxation-time Boltzmann treatment gives a finite anisotropy, while the Green-function calculation with vertex corrections gives a different result and even changes the sign of the effect in the weak- and intermediate-field range. Thus, the relaxation-time step is not innocuous in the Rashba-Zeeman problem with short-range disorder.

The present calculation gives a definite answer for the protected diagonal short-range scalar sector. In the continuum two-sheet quasiclassical model, a finite AMR cannot be obtained from a branch-dependent scalar Born lifetime. The spin-vector part of the on-shell Born self-energy is zero by the density Ward identity, and the projected scalar lifetime is therefore τ_0 . A finite AMR also cannot be obtained from the deformation of the two helicity Fermi contours. Once the impurity ladder is included, the anomalous Rashba velocity is cancelled, the dressed current vertex becomes the parabolic one, and the diagonal intraband Kubo integral reduces to the total occupied area.

This comparison separates two parts of Ref. [2]. The part confirmed here is the strong ladder cancellation of the anomalous Rashba velocity: in the weak-field metallic regime Raimondi *et al.* already found that the dressed retarded-advanced current vertex is approximately the parabolic vertex. The present derivation strengthens this statement by showing that the cancellation follows from the same area-Ward structure that controls the lifetime and the conductivity. The part not supported by the protected quasiclassical sector is the interpretation of a finite short-range-disorder AMR as a consequence of a field-dependent scalar transport time or of the diagonal two-sheet intraband contribution.

The finite AMR obtained numerically in Ref. [2] should therefore not be identified with the diagonal two-sheet quasiclassical contribution isolated here. Their numerical calculation treats a broader finite-broadening problem and displays its strongest structure near the spin-

polarization scale, where the Zeeman energy is of order the Fermi energy. In this regime the calculation no longer isolates the protected two-sheet diagonal quasiclassical sector. Raimondi *et al.* also discuss interband terms and the overlap of disorder-broadened subbands; such contributions are outside the area identity that fixes the leading diagonal intraband conductivity considered in the present work.

The likely technical origin of the spurious scalar-lifetime contribution is visible in relaxation-time treatments. If the angular density of states is evaluated on the field-deformed Fermi contour while the spin-overlap factor is evaluated on a reference contour, one obtains an apparent anisotropic relaxation time. Section S2 of the Supplemental Material shows this explicitly. The missing on-shell correction to the spin texture cancels that term. In other words, the density of states and the spin projector must be evaluated on the same helicity Fermi sheet. Once this is done, the projected scalar lifetime is τ_0 and carries no angular or field dependence.

The relation to Inoue *et al.* [3] is indirect but important. Their work concerns the anomalous Hall conductivity of a spin-polarized Rashba model, not the longitudinal AMR considered here. Nevertheless, it identifies the same kind of cancellation structure: for short-range disorder, the intrinsic Hall response is removed by the self-consistent vertex correction unless the quasiparticle lifetime is spin dependent. Kato *et al.* [4] formulated the corresponding criterion for intrinsic AMR. The Ward identity derived here shows that the required spin dependence of the projected Born lifetime is absent in the continuum two-sheet Rashba–Zeeman model. The spin-vector part of the on-shell Born self-energy is identically zero, so the cancellation criterion is satisfied and the diagonal AMR vanishes.

The numerical results of Wang and Pang [6] and Wang [7] should be read in a precise sense. They establish vanishing AMR for point-like nonmagnetic disorder in the two-band regime. Their plotted quantities test angular anisotropy under rotation of the magnetization; they do not formulate the stronger statement derived here, namely that the diagonal two-sheet quasiclassical conductivity itself is independent of the in-plane Zeeman field. The present result therefore goes beyond their delta-disorder AMR cancellation, but is fully consistent with it.

Those works also identify the mechanisms that evade the cancellation. For finite-range or remote scalar disorder, the Born self-energy contains a momentum-dependent kernel rather than the fully integrated spectral matrix. A quasiparticle then samples the spin spectral weight of final states with an angle-dependent form factor. The Ward identity constrains the unweighted spectral integral, not this momentum-filtered one. Therefore, finite-range or remote impurity scattering can generate a genuine angle-dependent transport time and finite AMR. This is precisely the distinction found in Refs. [6–8]: zero AMR for point-like nonmagnetic disorder in the two-

band regime and nonzero AMR for long-range disorder. Wang [7] also emphasized that the short-range cancellation no longer applies when only one helicity band is occupied, and that step-like structures appear near the singular magnetization where the density of states changes nonanalytically. These regimes are outside the two-sheet quasiclassical sector considered here.

The bilinear-magnetoresistance theory of Vaz *et al.* [9] is relevant for a different reason. Their experimental oxide system is more complex than the present single-band continuum model, but the microscopic single-band part of their theory uses local scalar disorder, a Born self-energy, and impurity vertex corrections. It then obtains a field-dependent relaxation-time structure and a quadratic magnetoresistance already for short-range disorder. The Ward identity derived here rules out that scalar-lifetime mechanism in the equilibrium single-band continuum model with delta-correlated disorder. The equilibrium Born self-energy has no spin-vector part, so it cannot generate the field-dependent scalar lifetime needed for such a quadratic response.

This statement separates the microscopic mechanism from the experimental phenomenology. It does not question the observation of bilinear magnetoresistance and a quadratic magnetoresistance in oxide heterostructures, where multiband physics, energy-dependent Rashba splittings, Lifshitz transitions, and finite-range disorder may all be present. It does, however, rule out the single-band point-like-disorder relaxation-time mechanism. If a finite quadratic magnetoresistance is obtained in a model that begins from the same continuum Rashba band and delta-correlated scalar disorder, its origin cannot be the equilibrium scalar Born lifetime or the diagonal area contribution derived here.

The comparison can be summarized sharply. Raimondi *et al.* correctly identified the ladder cancellation of the anomalous Rashba velocity, but their finite numerical AMR belongs to a broader finite-broadening/high-field calculation and should not be interpreted as the protected diagonal two-sheet quasiclassical contribution. Wang and Pang’s zero-AMR result for delta-function disorder is the correct short-range-disorder result for the angular anisotropy in this sector. Their nonzero AMR for remote impurities is a different finite-range-disorder mechanism, and Wang’s nonzero short-range AMR in the single-band regime is outside the two-sheet problem. The short-range-disorder scalar-lifetime mechanism invoked in analytical treatments that produce a field-dependent relaxation time is incorrect for the continuum two-sheet Rashba–Zeeman model. The reason is not a small numerical cancellation, but an exact Ward-identity and occupied-area cancellation within the stated quasiclassical problem.

VI. CONCLUSION

We have reexamined the quasiclassical short-range-disorder contribution to anisotropic magnetoresistance in a continuum Rashba film with an in-plane Zeeman field. The result is simple: point-like nonmagnetic impurities do not produce AMR in the leading quasiclassical conductivity of the two-sheet Rashba–Zeeman model. The projected scalar Born lifetime is isotropic and field independent because the spin-vector part of the on-shell spectral weight is fixed by a density Ward identity and the two-sheet occupied area is independent of the in-plane field. The same area identity controls the diagonal intra-band Kubo conductivity once the impurity ladder cancels the anomalous Rashba velocity and leaves the parabolic current vertex.

This resolves the controversy at the level of the quasiclassical mechanism considered here. A calculation that produces a field-dependent scalar relaxation time from point-like scalar disorder has either not evaluated the on-shell density-of-states and spin-overlap factors consistently, or has left the diagonal quasiclassical sector.

The analysis also makes precise why short-range disorder is the protected case. For point-like impurities, the Born self-energy is the full momentum-integrated spectral matrix. Its spin-vector part is then tied by the density Ward identity to the area invariant and vanishes; the same invariant closes the conductivity integral. Finite-range or remote scattering instead probes a momentum-filtered spectral matrix, on which the identity places no constraint and which can sustain a genuine angle-dependent transport time. Within the symmetric spin-vector sector, the dressed current vertex is, in addition, the complete ladder solution rather than a scalar truncation. A finite AMR is therefore a genuine signature of physics outside this protected short-range quasiclassical sector—finite-range scattering, inter-band mixing, additional band structure, or quantum effects beyond quasiclassics—measured against the field-independent baseline established here.

ACKNOWLEDGMENTS

A. K. gratefully acknowledges the hospitality of the KIT, Karlsruhe, during his scientific visit.

APPENDIX

Appendix A: Area identity for the two-sheet Rashba spectrum

Here we prove the geometric identity used in Sec. III B. The proof is carried out in the continuum parabolic model, with both helicity sheets included, and in the

weak-spin-orbit regime

$$\lambda = m\alpha < R = \sqrt{2m\mu}. \quad (\text{A1})$$

We also assume that the $s = +$ sheet is occupied, $B < \mu$. This is the two-sheet regime used throughout the main calculation. Within this domain, the total occupied area at fixed chemical potential is independent of the in-plane Zeeman field. This is the geometric input that makes the spin-vector part of the on-shell Born self-energy vanish.

We align the x -axis with \mathbf{B} and write

$$\mathbf{p} = p(\cos\theta, \sin\theta), \quad b = \frac{B}{\alpha}. \quad (\text{A2})$$

The Fermi-contour equation for branch $s = \pm$ becomes

$$p_s^2 + 2s\lambda\sqrt{p_s^2 + 2bp_s\cos\theta + b^2} = R^2. \quad (\text{A3})$$

In the two-sheet regime each branch has a single positive outer radius $p_s(\theta)$ for every direction θ , so the occupied area is

$$A_{\text{tot}}^{(p)} = \frac{1}{2} \int_0^{2\pi} d\theta [p_+^2(\theta) + p_-^2(\theta)]. \quad (\text{A4})$$

To evaluate this area, we square Eq. (A3) obtaining

$$p^4 - (2R^2 + 4\lambda^2)p^2 - 8\lambda^2b\cos\theta p + (R^4 - 4\lambda^2b^2) = 0. \quad (\text{A5})$$

We first justify the root counting used below. The $+$ branch has one positive root. Its radial dispersion

$$\epsilon_+(p, \theta) = \frac{p^2}{2m} + \alpha\sqrt{p^2 + 2bp\cos\theta + b^2} \quad (\text{A6})$$

is strictly convex in p :

$$\frac{d^2\epsilon_+}{dp^2} = \frac{1}{m} + \alpha \frac{b^2 \sin^2\theta}{(p^2 + 2bp\cos\theta + b^2)^{3/2}} > 0. \quad (\text{A7})$$

The second term is non-negative and the first term is strictly positive. For $\theta = \pi$, the function $\epsilon_+(p, \pi) = p^2/(2m) + \alpha|p - b|$ has a kink at $p = b$ (the Rashba degeneracy point on the Fermi surface), where the formula for $d^2\epsilon_+/dp^2$ is undefined. On each smooth piece, $d^2\epsilon_+/dp^2 = 1/m > 0$; moreover, ϵ_+ is the sum of two convex functions and is therefore globally convex. The root-counting conclusion is unchanged. Since $\epsilon_+(0, \theta) = B < \mu$ in the two-sheet regime and $\epsilon_+(p, \theta) \rightarrow +\infty$ as $p \rightarrow \infty$, the equation $\epsilon_+(p, \theta) = \mu$ has exactly one positive solution. We denote it by $p_+(\theta)$.

The $-$ branch also has one positive outer root. Any solution of $\epsilon_-(p, \theta) = \mu$ satisfies

$$\frac{p^2}{2m} = \mu + \alpha\sqrt{p^2 + 2bp\cos\theta + b^2} > \mu, \quad (\text{A8})$$

and therefore lies at $p > R$. Moreover,

$$\left| \frac{d}{dp} \sqrt{p^2 + 2bp\cos\theta + b^2} \right| = \frac{|p + b\cos\theta|}{\sqrt{p^2 + 2bp\cos\theta + b^2}} \leq 1, \quad (\text{A9})$$

because $(p + b \cos \theta)^2 \leq p^2 + 2bp \cos \theta + b^2$, with the difference equal to $b^2 \sin^2 \theta \geq 0$. Hence

$$\frac{d\epsilon_-}{dp} = \frac{p}{m} - \alpha \frac{p + b \cos \theta}{\sqrt{p^2 + 2bp \cos \theta + b^2}} \geq \frac{p}{m} - \alpha. \quad (\text{A10})$$

For $p > R$, and in the weak-spin-orbit regime $m\alpha/R < 1$, this gives

$$\frac{d\epsilon_-}{dp} > \frac{R}{m} - \alpha > 0. \quad (\text{A11})$$

Thus $\epsilon_-(p, \theta)$ is strictly increasing on the interval where any root can occur. Since

$$\epsilon_-(R, \theta) = \mu - \alpha \sqrt{R^2 + 2bR \cos \theta + b^2} < \mu \quad (\text{A12})$$

except at the isolated point where the square root vanishes, and since $\epsilon_-(p, \theta) \rightarrow +\infty$, the equation $\epsilon_-(p, \theta) = \mu$ has exactly one positive solution. We denote it by $p_-(\theta)$.

It remains to identify the negative roots of the quartic. Substituting $p \rightarrow -p$ in Eq. (A5) changes only the sign of the linear term, $-8\lambda^2 b \cos \theta p$, and leaves all other terms unchanged. This is the same transformation as replacing $\cos \theta \rightarrow -\cos \theta = \cos(\theta + \pi)$. Therefore a positive root $p_s(\theta + \pi)$ of the quartic at angle $\theta + \pi$ gives a negative root $-p_s(\theta + \pi)$ of the quartic at angle θ . The four roots of the quartic at fixed θ are therefore

$$p_+(\theta), p_-(\theta), -p_+(\theta + \pi), -p_-(\theta + \pi). \quad (\text{A13})$$

Let

$$S(\theta) = p_+^2(\theta) + p_-^2(\theta). \quad (\text{A14})$$

The four roots of Eq. (A5) have squared sum $S(\theta) + S(\theta + \pi)$. The quartic has no cubic term. If its roots are r_i , then $\sum_i r_i = 0$, and Vieta's relation gives

$$\sum_{i < j} r_i r_j = -(2R^2 + 4\lambda^2). \quad (\text{A15})$$

Using

$$\left(\sum_i r_i \right)^2 = \sum_i r_i^2 + 2 \sum_{i < j} r_i r_j = 0, \quad (\text{A16})$$

we obtain

$$\sum_i r_i^2 = S(\theta) + S(\theta + \pi) = 4R^2 + 8\lambda^2. \quad (\text{A17})$$

Integrating Eq. (A17) over θ gives

$$A_{\text{tot}}^{(p)} = \frac{1}{2} \int_0^{2\pi} d\theta S(\theta) = 2\pi (R^2 + 2\lambda^2). \quad (\text{A18})$$

This result contains no $b = B/\alpha$, thus $\partial A_{\text{tot}}^{(p)}/\partial b = 0$.

Since the particle density is

$$n(\mu, \mathbf{B}) = \frac{A_{\text{tot}}^{(p)}}{(2\pi)^2}, \quad (\text{A19})$$

we obtain

$$\frac{\partial n(\mu, \mathbf{B})}{\partial \mathbf{B}} = 0. \quad (\text{A20})$$

The identity is exact in the continuum parabolic two-sheet model used throughout: a quadratic kinetic dispersion with no lattice cutoff and both helicity sheets retained in the two-sheet regime $B < \mu$. The field independence is the constancy of the quartic root sum in Eq. (A17), which combines the two sheets, and it is precisely this two-sheet continuum structure that fixes the spin-vector part of the on-shell Born self-energy through $\partial n/\partial \mathbf{B}$.

Appendix B: Velocity operator vertex correction

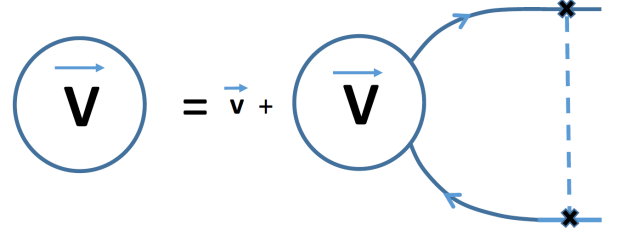


Figure 1. Diagram for the velocity vertex function.

1. Exact quasiclassical ladder solution

We derive the current vertex within the same two-sheet diagonal quasiclassical framework that is used in the main text for the lifetime and the conductivity. Both helicity branches are assumed to cross the chemical potential, and the local helicity splitting on the Fermi contours is resolved compared with the elastic broadening, so that the diagonal helicity projection is controlled. No expansion in B/E_F or $\alpha p_F/E_F$ is needed in the derivation below. The ratio $\gamma = B/(\alpha p_F)$ is arbitrary within this two-sheet regime. The lifetime entering this appendix is the scalar Born lifetime τ_0 derived in Sec. III. The diagram for the velocity vertex function is shown in Fig. 1, where the dotted line between two crosses corresponds to the factor $1/(m\tau_0)$.

It is useful to prove the vertex identity in a slightly more general notation. We temporarily write the linear spin-orbit field as

$$d_j(\mathbf{p}) = \mathbf{A}_{ji} p_i + B_j, \quad (\text{B1})$$

where repeated Cartesian indices are summed. The Rashba–Zeeman model used in the main text is obtained by setting $A_{ji} = \alpha\delta_{ji}$ in the rotated in-plane spin basis used there. In an unrotated Rashba convention, the same formulas hold with the corresponding fixed in-plane rotation included in \mathbf{A} . We also introduce a temporary scalar tilt $\mathbf{u} \cdot \mathbf{p}$ and set $\mathbf{u} = 0$ after differentiating the occupied area. Thus,

$$\varepsilon_s(\mathbf{p}) = \frac{p^2}{2m} + \mathbf{u} \cdot \mathbf{p} + sd(\mathbf{p}), \quad d(\mathbf{p}) = |\mathbf{d}(\mathbf{p})|, \quad s = \pm. \quad (\text{B2})$$

At $\mathbf{u} = 0$, the two helicity Fermi contours are written as

$$\hat{\Gamma}_i(\mathbf{p}) = \hat{v}_i(\mathbf{p}) + \sum_{s=\pm} \int_0^{2\pi} \frac{d\phi}{2\pi} \frac{p_s}{4D_s} (1 + s\boldsymbol{\nu}_s \cdot \hat{\boldsymbol{\sigma}}) \hat{\Gamma}_i(p_s \mathbf{e}_\phi) (1 + s\boldsymbol{\nu}_s \cdot \hat{\boldsymbol{\sigma}}), \quad (\text{B6})$$

where

$$\hat{v}_i(\mathbf{p}) = \frac{p_i}{m} \hat{I} + A_{ji} \hat{\sigma}_j \quad (\text{B7})$$

is the bare velocity operator. We now show that

$$\hat{\Gamma}_i(\mathbf{p}) = \frac{p_i}{m} \hat{I} \quad (\text{B8})$$

solves Eq. (B6) exactly within the two-sheet diagonal quasiclassical projection.

Substituting Eq. (B8) into the ladder correction in Eq. (B6) gives

$$\begin{aligned} \hat{\mathcal{L}}_i &= \sum_{s=\pm} \int_0^{2\pi} \frac{d\phi}{2\pi} \frac{p_s^2 e_{\phi,i}}{2mD_s} (1 + s\boldsymbol{\nu}_s \cdot \hat{\boldsymbol{\sigma}}) \\ &= \mathcal{L}_i^{(0)} \hat{I} + \mathcal{L}_{ij}^{(\sigma)} \hat{\sigma}_j, \end{aligned} \quad (\text{B9})$$

with

$$\mathcal{L}_i^{(0)} = \sum_{s=\pm} \int_0^{2\pi} \frac{d\phi}{2\pi} \frac{p_s^2 e_{\phi,i}}{2mD_s}, \quad (\text{B10})$$

$$\mathcal{L}_{ij}^{(\sigma)} = \sum_{s=\pm} \int_0^{2\pi} \frac{d\phi}{2\pi} \frac{sp_s^2 e_{\phi,i} \nu_{s,j}}{2mD_s}. \quad (\text{B11})$$

The two angular identities needed to evaluate these coefficients are Fermi-sea Ward identities. Let

$$A_{\text{tot}}(\mu, \mathbf{A}, \mathbf{B}, \mathbf{u}) = \frac{1}{2} \sum_{s=\pm} \int_0^{2\pi} d\phi p_s^2(\phi) \quad (\text{B12})$$

be the total occupied area of the two helicity sheets. For $\mathbf{u} = 0$, the two-sheet continuum area is

$$A_{\text{tot}}(\mu, \mathbf{A}, \mathbf{B}, 0) = 4\pi m\mu + 2\pi m^2 \text{tr} \mathbf{A}^T \mathbf{A}. \quad (\text{B13})$$

$p_s(\phi) \mathbf{e}_\phi$ and obey

$$\mu = \frac{p_s^2}{2m} + sd_s, \quad d_s = |\mathbf{A}p_s \mathbf{e}_\phi + \mathbf{B}|. \quad (\text{B3})$$

We denote the corresponding spin direction by

$$\nu_{s,j}(\phi) = \frac{A_{ji} p_s e_{\phi,i} + B_j}{d_s}, \quad (\text{B4})$$

and define

$$D_s(\phi) = p_s + sm \nu_{s,j} A_{ji} e_{\phi,i} = m \left. \frac{\partial \varepsilon_s}{\partial p} \right|_{p=p_s(\phi), \mathbf{u}=0}. \quad (\text{B5})$$

After the radial integration of the retarded–advanced bubble, the point-disorder ladder equation for the current vertex takes the form

This is the same area identity as in Appendix S3, written for a general linear spin-orbit tensor. In particular, it is independent of \mathbf{B} but has a fixed quadratic dependence on the spin-orbit tensor.

First, differentiate the area with respect to the temporary tilt u_i . Equivalently, shift $\mathbf{q} = \mathbf{p} + m\mathbf{u}$. This gives

$$A_{\text{tot}}(\mu, \mathbf{A}, \mathbf{B}, \mathbf{u}) = A_{\text{tot}}\left(\mu + mu^2/2, \mathbf{A}, \mathbf{B} - m\mathbf{A}\mathbf{u}, 0\right), \quad (\text{B14})$$

so the derivative at $\mathbf{u} = 0$ vanishes. Differentiating the on-shell condition gives

$$\left. \frac{\partial p_s}{\partial u_i} \right|_{\mathbf{u}=0} = -\frac{mp_s e_{\phi,i}}{D_s}, \quad (\text{B15})$$

and therefore

$$0 = \left. \frac{\partial A_{\text{tot}}}{\partial u_i} \right|_{\mathbf{u}=0} = -m \sum_{s=\pm} \int_0^{2\pi} d\phi \frac{p_s^2 e_{\phi,i}}{D_s}. \quad (\text{B16})$$

Equation (B16) gives

$$\mathcal{L}_i^{(0)} = 0. \quad (\text{B17})$$

Second, differentiate Eq. (B13) with respect to A_{ji} . From the explicit area identity,

$$\frac{\partial A_{\text{tot}}}{\partial A_{ji}} = 4\pi m^2 A_{ji}. \quad (\text{B18})$$

On the other hand, differentiating the on-shell condition Eq. (B3) at fixed μ gives

$$\left. \frac{\partial p_s}{\partial A_{ji}} \right|_{\mu} = -\frac{msp_s e_{\phi,i} \nu_{s,j}}{D_s}, \quad (\text{B19})$$

and hence

$$\frac{\partial A_{\text{tot}}}{\partial A_{ji}} = -m \sum_{s=\pm} \int_0^{2\pi} d\phi \frac{sp_s^2 e_{\phi,i} \nu_{s,j}}{D_s}. \quad (\text{B20})$$

Comparing Eqs. (B18) and (B20), and using Eq. (B11), gives

$$\mathcal{L}_{ij}^{(\sigma)} = -A_{ji}. \quad (\text{B21})$$

Thus, the ladder correction generated by the trial vertex Eq. (B8) is

$$\hat{\mathcal{L}}_i = -A_{ji} \hat{\sigma}_j. \quad (\text{B22})$$

It cancels the anomalous part of the bare velocity in Eq. (B7). The exact diagonal quasiclassical current vertex is therefore

$$\hat{\Gamma}_i(\mathbf{p}) = \frac{p_i}{m} \hat{I}. \quad (\text{B23})$$

For the Rashba convention of the main text this is the vector statement

$$\mathbf{V} = \frac{\mathbf{p}}{m}. \quad (\text{B24})$$

2. Coherence with the density Ward identity

The derivation above makes the structure of the calculation coherent with the main text. The scalar Born lifetime is fixed by the derivative of the same two-sheet area with respect to the Zeeman field: since A_{tot} is independent of \mathbf{B} , the spin-vector part of the momentum-integrated on-shell spectral weight vanishes. The current vertex is fixed by two neighboring derivatives of the same Fermi-sea identity. The derivative with respect to the scalar tilt \mathbf{u} removes any scalar ladder correction to the current, while the derivative with respect to the spin-orbit tensor \mathbf{A} gives exactly the negative of the anomalous velocity. Thus, the cancellation of the Rashba velocity in Eq. (B23) and the field independence of the scalar lifetime are not separate accidents. They are two Ward-identity consequences of the same two-sheet area invariant.

This is also why the vertex correction is naturally obtained at the same level of approximation as the conductivity calculation. No high-density expansion is involved. The assumptions are precisely those used in the diagonal quasiclassical Kubo formula: point-like scalar disorder, parabolic dispersion, a linear-in-momentum spin-orbit field, two occupied helicity sheets, and a resolved local helicity splitting on the Fermi contours.

3. Why the transport vertex is essential for the area reduction

The area reduction is not a property of the bare band structure alone. It also relies on the ladder renormalization of the current vertex. A naive argument would miss

this point. Even for point-like scalar disorder, the projected scattering probability contains the helicity coherence factor appearing in Eq. (18). This factor makes the effective transport kernel angular dependent even when the bare impurity amplitude is momentum independent. Thus, the transport vertex is nontrivial. The exact quasiclassical ladder calculation above cancels the anomalous spin-orbit velocity even in the presence of Zeeman field, leaving the parabolic current vertex used in Sec. IV. This agrees with the strong ladder cancellation of the anomalous velocity discussed by Raimondi *et al.* [2].

This renormalization is precisely what allows the conductivity integral to close onto the Fermi-sea area. With the dressed current vertex $\hat{V}_x = (\mathbf{p}/m)_x$ on one side of the retarded-advanced bubble and the band velocity $v_{s,x}$ on the other side, the branch integrand becomes Eq. (39). The term containing $\partial_\phi p_s$ then integrates by parts, giving Eq. (41) and finally the area form Eq. (42). If the anomalous velocity were instead kept on the dressed leg, so that the bare band velocity $v_{s,x}$ were used on both sides of the bubble, the integrand would acquire the additional term

$$p_s \frac{v_{s,x}^2}{v_{s,\parallel}} - p_s \frac{p_x v_{s,x}}{m v_{s,\parallel}} = s\alpha p_s \nu_x^{(s)}(\phi) \left[\cos \phi + \frac{\sin \phi}{p_s} \frac{\partial p_s}{\partial \phi} \right]. \quad (\text{B25})$$

Here, Eq. (38) has been used and $\nu_x^{(s)}(\phi) = \boldsymbol{\nu}^{(s)}(\phi) \cdot \mathbf{e}_x$. This factor is explicitly field dependent through the on-shell spin texture $\boldsymbol{\nu}^{(s)}(\phi)$. The term in Eq. (B25) is not the total-derivative contribution that appears in the geometric reduction, and it does not combine with $\partial_\phi(p_s^2)$ to produce the field-independent two-sheet area.

Thus, the absence of diagonal AMR in Sec. IV is not just a consequence of the bare impurity amplitude being isotropic. It is a consequence of the transport vertex: the ladder removes the anomalous spin-orbit velocity from the current vertex, and this removal is what allows the contour integral to reduce to the field-independent total area.

4. Completeness of the dressed current vertex

The exact calculation in Sec. B 1 gives the dressed current vertex $\mathbf{V} = \mathbf{p}/m$ by cancelling the spin-orbit part of the bare velocity. We now record the complementary uniqueness statement in the symmetric spin-vector sector that controls the longitudinal conductivity. This statement rules out an additional homogeneous spin-vector vertex and shows that \mathbf{p}/m is the complete current vertex in this sector.

A spin-vector correction to the current vertex has the form $\delta V_k = b_{kj} \hat{\sigma}_j$, with the tensor b_{kj} built from the identity and the preferred in-plane direction \mathbf{e}_B . Its symmetric part is spanned by δ_{kj} and $e_{B,k} e_{B,j}$. The antisymmetric part $\propto \epsilon_{kj}$ belongs to the transverse sector and does not contribute to the longitudinal anisotropy

$\sigma_{xx} - \sigma_{yy}$; the mixed symmetric structure $e_{B,k}\hat{e}_{\perp,j}$, with $\hat{e}_{\perp} = \hat{z} \times \mathbf{e}_B$, is odd under reflection about \mathbf{e}_B and is likewise excluded. The general symmetric spin-vector correction relevant to the AMR is therefore

$$\delta\mathbf{V} = \beta\hat{\sigma} + \rho\mathbf{e}_B(\mathbf{e}_B \cdot \hat{\sigma}), \quad (\text{B26})$$

an isotropic Rashba-like term and a field-aligned term.

The homogeneous equation for such an additional vertex is obtained by subtracting the particular solution Eq. (B24) from the Bethe–Salpeter equation. In the same diagonal quasiclassical sector it reads

$$\delta\mathbf{V} = \sum_{s=\pm} \int_0^{2\pi} \frac{d\phi}{2\pi} \frac{p_s}{4D_s} (1 + s\boldsymbol{\nu}_s \cdot \hat{\sigma}) \delta\mathbf{V} (1 + s\boldsymbol{\nu}_s \cdot \hat{\sigma}), \quad (\text{B27})$$

with p_s , D_s , and $\boldsymbol{\nu}_s$ defined in Eqs. (B3)–(B5). Choosing axes with $\mathbf{e}_B = \hat{x}$, the transverse component is $\delta V_y = \beta\hat{\sigma}_y$. Projecting the y component of Eq. (B27) onto $\hat{\sigma}_y$ gives

$$\beta \left[1 - \sum_{s=\pm} \int_0^{2\pi} \frac{d\phi}{2\pi} \frac{p_s}{2D_s} \nu_{s,y}^2 \right] = 0. \quad (\text{B28})$$

Write $\Sigma_a = \sum_s \int_0^{2\pi} \frac{d\phi}{2\pi} \frac{p_s}{2D_s} \nu_{s,a}^2$ for $a = x, y$, so the bracket in Eq. (B28) is $1 - \Sigma_y$. Since $\nu_{s,x}^2 + \nu_{s,y}^2 = 1$,

$$\Sigma_x + \Sigma_y = \sum_s \int_0^{2\pi} \frac{d\phi}{2\pi} \frac{p_s}{2D_s} = \frac{\pi}{m} \frac{\partial n}{\partial \mu} = 1, \quad (\text{B29})$$

where the last step uses $n = m\mu/\pi + m^2\alpha^2/\pi$ from the area identity. The bracket therefore equals Σ_x , which is strictly positive (the integrand is non-negative and not identically zero), and $\beta = 0$. With $\beta = 0$, the field-aligned component is $\delta V_x = \rho\hat{\sigma}_x$. Projection of the x component onto $\hat{\sigma}_x$ gives the analogous equation

$$\rho \left[1 - \sum_{s=\pm} \int_0^{2\pi} \frac{d\phi}{2\pi} \frac{p_s}{2D_s} \nu_{s,x}^2 \right] = 0, \quad (\text{B30})$$

whose bracket equals $1 - \Sigma_x = \Sigma_y > 0$ by Eq. (B29). Hence $\rho = 0$, and $\beta = \rho = 0$.

The homogeneous ladder equation therefore has no spin-vector solution in the symmetric sector relevant to the longitudinal conductivity. The area reduction of Sec. IV rests on the complete current vertex; the absence of AMR is not a consequence of restricting the vertex to a scalar form.

-
- [1] W. Thomson (Lord Kelvin), *On the electro-dynamic qualities of metals*, Proc. R. Soc. London **8**, 546 (1857).
- [2] R. Raimondi, M. Leadbeater, P. Schwab, E. Caroti, and C. Castellani, Spin-orbit induced anisotropy in the magnetoconductance of two-dimensional metals, Phys. Rev. B **64**, 235110 (2001).
- [3] J.-I. Inoue, T. Kato, Y. Ishikawa, H. Itoh, G. E. W. Bauer, and L. W. Molenkamp, Vertex Corrections to the Anomalous Hall Effect in Spin-Polarized Two-Dimensional Electron Gases with a Rashba Spin-Orbit Interaction, Phys. Rev. Lett. **97**, 046604 (2006).
- [4] T. Kato, Y. Ishikawa, H. Itoh, and J.-I. Inoue, Intrinsic anisotropic magnetoresistance in spin-polarized two-dimensional electron gas with Rashba spin-orbit interaction, Phys. Rev. B **77**, 233404 (2008).
- [5] M. Trushin, K. Výborný, P. Moraczewski, A. A. Kovalev, J. Schliemann, and T. Jungwirth, Anisotropic magnetoresistance of spin-orbit coupled carriers scattered from polarized magnetic impurities, Phys. Rev. B **80**, 134405 (2009).
- [6] C. M. Wang and M. Q. Pang, Nonvanishing anisotropic magnetoresistance in Rashba two-dimensional electron systems with nonmagnetic disorders, EPL **88**, 27005 (2009).
- [7] C. M. Wang, Anisotropic magnetoresistance in a two-dimensional electron system with Rashba and Dresselhaus spin-orbit coupling, Phys. Rev. B **82**, 165331 (2010).
- [8] C. M. Wang, Anisotropic magnetoresistance in a Rashba two-dimensional electron system: The role of nonmagnetic long-range scattering and nonparabolic energy band, EPL **93**, 17005 (2011).
- [9] D. C. Vaz, F. Trier, A. Dyrdał, A. Johansson, K. Garcia, A. Barthélémy, I. Mertig, J. Barnaś, A. Fert, and M. Bibes, Determining the Rashba parameter from the bilinear magnetoresistance response in a two-dimensional electron gas, Phys. Rev. Materials **4**, 071001(R) (2020).
- [10] P. Štředa, Theory of quantised Hall conductivity in two dimensions, J. Phys. C: Solid State Phys. **15**, L717 (1982).
- [11] See Supplemental Material for technical details: the projected Dyson-equation derivation of the branch-resolved lifetime, a perturbative weak-field check showing where an apparent anisotropic scalar lifetime enters and why it cancels, and a complementary shifted-coordinate proof of the two-sheet area identity.

Supplemental Information

This Supplemental Material provides three supporting derivations for the main text. Section S1 gives the projected Dyson-equation derivation of the branch-resolved lifetime. Section S2 gives a perturbative weak-field check showing where an apparent anisotropic scalar lifetime enters and why it cancels. Section S3 gives an alternative shifted-coordinate proof of the two-sheet area identity.

Appendix S1: Projected Dyson equation and generic branch-dependent lifetime

This section gives the matrix derivation behind Sec. III of the main text. The main text uses the final scalar result $\tau_s(\phi) = \tau_0$, but the intermediate steps are useful for two reasons. First, they show how an angle-dependent lifetime would arise in a generic spin-orbit model. Second, they make clear why the short-range Rashba cancellation is nontrivial rather than a consequence of momentum-independent disorder alone.

1. Born self-energy and radial integral

The helicity projectors are

$$\hat{\Omega}_s(\mathbf{p}) = \frac{1 + s\boldsymbol{\nu}_\mathbf{p} \cdot \hat{\boldsymbol{\sigma}}}{2}, \quad \boldsymbol{\nu}_\mathbf{p} = \frac{\alpha\mathbf{p} + \mathbf{B}}{|\alpha\mathbf{p} + \mathbf{B}|}. \quad (\text{S1})$$

The clean retarded Green's function is

$$\hat{G}^{R,0}(\epsilon, \mathbf{p}) = \frac{\hat{\Omega}_+(\mathbf{p})}{\epsilon - \epsilon_+(\mathbf{p}) + i0^+} + \frac{\hat{\Omega}_-(\mathbf{p})}{\epsilon - \epsilon_-(\mathbf{p}) + i0^+}. \quad (\text{S2})$$

For δ -correlated scalar disorder,

$$\hat{\Sigma}^R(\epsilon) = n_{\text{imp}}|U|^2 \int \frac{d^2p'}{(2\pi)^2} \hat{G}^{R,0}(\epsilon, \mathbf{p}'). \quad (\text{S3})$$

It is independent of the external momentum, but it is a spin matrix.

At fixed angle ϕ' , the radial integral on branch s' is evaluated by changing variables to $\xi = \epsilon_{s'}(p', \phi') - \mu$. On the Fermi surface,

$$p' dp' = \frac{p_{s'}(\phi')}{v_{s',\parallel}(\phi')} d\xi, \quad (\text{S4})$$

where

$$v_{s,\parallel}(\phi) = \left. \frac{\partial \epsilon_s(p, \phi)}{\partial p} \right|_{p=p_s(\phi)}, \quad \rho_s(\phi) = \frac{p_s(\phi)}{2\pi v_{s,\parallel}(\phi)}. \quad (\text{S5})$$

Extending the ξ integration to the full real axis gives

$$\begin{aligned} \int_0^\infty \frac{p' dp'}{2\pi} \frac{\hat{\Omega}_{s'}(\phi')}{\mu - \epsilon_{s'}(p', \phi') + i0^+} &= -\rho_{s'}(\phi') \int_{-\infty}^\infty \frac{d\xi}{\xi - i0^+} \hat{\Omega}_{s'}(\phi') \\ &= -i\pi \rho_{s'}(\phi') \hat{\Omega}_{s'}(\phi') + \text{principal value}. \end{aligned} \quad (\text{S6})$$

The principal value contributes to $\text{Re } \Sigma^R$. The on-shell imaginary part is therefore

$$-\text{Im } \hat{\Sigma}^R(\mu) = \pi n_{\text{imp}}|U|^2 \sum_{s=\pm} \int \frac{d^2p}{(2\pi)^2} \delta(\mu - \epsilon_s(\mathbf{p})) \hat{\Omega}_s(\mathbf{p}). \quad (\text{S7})$$

2. Projection of the Dyson equation

We now project the Dyson equation onto the local helicity basis at the external momentum $\mathbf{p} = p\mathbf{e}_\phi$. For any operator \hat{A} , define

$$A_{ss'}(\phi) = \langle s, \phi | \hat{A} | s', \phi \rangle. \quad (\text{S8})$$

Although $\hat{\Sigma}^R$ is momentum independent, its matrix elements $\Sigma_{ss'}(\phi)$ depend on ϕ , because the basis states $|s, \phi\rangle$ rotate with the local spin texture.

The inverse Green's function in this basis is

$$[(G^R)^{-1}(\phi)]_{ss'} = [\epsilon - \epsilon_s(\phi)]\delta_{ss'} - \Sigma_{ss'}(\phi), \quad (\text{S9})$$

or

$$(G^R)^{-1} = \begin{pmatrix} \epsilon - \epsilon_+(\phi) - \Sigma_{++}(\phi) & -\Sigma_{+-}(\phi) \\ -\Sigma_{-+}(\phi) & \epsilon - \epsilon_-(\phi) - \Sigma_{--}(\phi) \end{pmatrix}. \quad (\text{S10})$$

Inverting this matrix gives

$$G_{ss}^R(\epsilon, \mathbf{p}) = \frac{\epsilon - \epsilon_{-s}(\phi) - \Sigma_{-s, -s}(\phi)}{\mathcal{D}(\phi)}, \quad (\text{S11})$$

$$G_{s, -s}^R(\epsilon, \mathbf{p}) = \frac{\Sigma_{s, -s}(\phi)}{\mathcal{D}(\phi)}, \quad (\text{S12})$$

with

$$\begin{aligned} \mathcal{D}(\phi) &= [\epsilon - \epsilon_+(\phi) - \Sigma_{++}(\phi)][\epsilon - \epsilon_-(\phi) - \Sigma_{--}(\phi)] \\ &\quad - \Sigma_{+-}(\phi)\Sigma_{-+}(\phi). \end{aligned} \quad (\text{S13})$$

Equivalently, the diagonal element may be written as

$$G_s^R(\epsilon, \mathbf{p}) = \frac{1}{\epsilon - \epsilon_s(\phi) - \Sigma_{ss}(\phi) - \frac{\Sigma_{s, -s}(\phi)\Sigma_{-s, s}(\phi)}{\epsilon - \epsilon_{-s}(\phi) - \Sigma_{-s, -s}(\phi)}}. \quad (\text{S14})$$

This expression separates two issues. The diagonal matrix element $\Sigma_{ss}(\phi)$ gives the branch-projected broadening and energy shift. The last term describes the effect of off-diagonal matrix elements in the local helicity basis.

The momentum independence of $\hat{\Sigma}^R$ does not imply that $\Sigma_{ss}(\phi)$ is angle independent. Write

$$\hat{\Sigma}^R = \Sigma_0 \hat{I} + \boldsymbol{\Sigma} \cdot \hat{\boldsymbol{\sigma}}. \quad (\text{S15})$$

Then,

$$\Sigma_{ss}(\phi) = \Sigma_0 + s \boldsymbol{\Sigma} \cdot \boldsymbol{\nu}^{(s)}(\phi). \quad (\text{S16})$$

Thus, a fixed spin matrix becomes angle dependent after projection onto a momentum-dependent helicity basis. In a generic spin-orbit model, a nonzero spin-vector part of the Born self-energy would produce an angle-dependent broadening. The Ward identity in Sec. III of the main text shows that this spin-vector part vanishes for the on-shell imaginary self-energy of the continuum short-range Rashba problem.

3. Golden-Rule limit and general branch-resolved rate

In the clean split-band regime,

$$\Delta(\phi)\tau_0 \gg 1, \quad \Delta(\phi) = 2|\alpha\mathbf{p} + \mathbf{B}| \quad (\text{S17})$$

on the Fermi surface, the off-diagonal correction in Eq. (S14) is small. Since $\Sigma \sim 1/\tau_0$, the last term in Eq. (S14) is of order $(1/\tau_0)^2/\Delta$, smaller than the diagonal broadening by $(\Delta\tau_0)^{-1}$. The diagonal Green's function then has the quasiparticle form

$$G_s^R(\epsilon, \mathbf{p}) \simeq \frac{1}{\epsilon - \epsilon_s(\mathbf{p}) - \text{Re} \Sigma_{ss}(\phi) + i\Gamma_s(\phi)}, \quad \Gamma_s(\phi) = -\text{Im} \Sigma_{ss}(\phi). \quad (\text{S18})$$

Projecting the on-shell Born spectral matrix gives

$$\frac{1}{\tau_s(\phi)} = 2\pi n_{\text{imp}} |U|^2 \sum_{s'=\pm} \int_0^{2\pi} \frac{d\phi'}{2\pi} \rho_{s'}(\phi') \frac{1 + ss' \boldsymbol{\nu}^{(s)}(\phi) \cdot \boldsymbol{\nu}^{(s')}(\phi')}{2}. \quad (\text{S19})$$

The overlap factor follows from

$$\text{tr} \left[\hat{\Omega}_s(\phi) \hat{\Omega}_{s'}(\phi') \right] = \frac{1 + ss' \boldsymbol{\nu}^{(s)}(\phi) \cdot \boldsymbol{\nu}^{(s')}(\phi')}{2}, \quad (\text{S20})$$

using $\text{tr}[\hat{\sigma}_i \hat{\sigma}_j] = 2\delta_{ij}$.

The spin texture in Eq. (S19) is the on-shell texture

$$\boldsymbol{\nu}^{(s)}(\phi) = \frac{\alpha p_s(\phi) \mathbf{e}_\phi + \mathbf{B}}{|\alpha p_s(\phi) \mathbf{e}_\phi + \mathbf{B}|}. \quad (\text{S21})$$

It should not be replaced by the texture evaluated at p_F unless the corresponding error is kept consistently.

It is useful to introduce

$$x_s(\phi) = \frac{p_s(\phi)}{p_F}, \quad \theta = \phi - \phi_B, \quad \varepsilon = \frac{m\alpha}{p_F}, \quad \gamma = \frac{B}{\alpha p_F}. \quad (\text{S22})$$

Then

$$\boldsymbol{\nu}^{(s)}(\phi) = \frac{x_s(\phi) \mathbf{e}_\phi + \gamma \mathbf{e}_B}{\sqrt{x_s^2 + 2\gamma x_s \cos \theta + \gamma^2}}. \quad (\text{S23})$$

The dimensionless on-shell equation is Eq. (S3). Solving perturbatively gives Eq. (S4). The angular density of states is

$$\rho_s(\phi) = \frac{m}{2\pi} \frac{x_s}{x_s + s\varepsilon \boldsymbol{\nu}_\mathbf{p} \cdot \mathbf{e}_\phi}. \quad (\text{S24})$$

Equations (S23)–(S24) show why the partially projected expansion is delicate. The branch-dependent shift of x_s modifies both the density of states and the spin texture. The terms that appear as an anisotropic density-of-states contribution are cancelled by the corresponding on-shell correction to $\boldsymbol{\nu}_\mathbf{p}$. The full expansion through the order needed for the conductivity calculation is given in Appendix S2. The nonperturbative Ward identity in Sec. III of the main text explains why this cancellation persists in the continuum two-sheet short-range model.

Appendix S2: Perturbative check of the scalar Born lifetime

This section gives a perturbative check of the scalar-lifetime cancellation derived nonperturbatively in Sec. III and Appendix A of the main text. The goal is not to rederive the Ward identity, but to show explicitly how an apparent anisotropic term is removed when all on-shell quantities are evaluated on the same helicity Fermi sheet.

The branch-resolved rate is

$$\frac{1}{\tau_s(\phi)} = 2\pi n_{\text{imp}} |U|^2 \sum_{s'=\pm} \int_0^{2\pi} \frac{d\phi'}{2\pi} \rho_{s'}(\phi') \frac{1 + ss' \boldsymbol{\nu}^{(s)}(\phi) \cdot \boldsymbol{\nu}^{(s')}(\phi')}{2}. \quad (\text{S1})$$

The spin texture in the overlap must be evaluated on the same Fermi sheet as the density of states:

$$\boldsymbol{\nu}^{(s)}(\phi) \equiv \boldsymbol{\nu}_\mathbf{p} \Big|_{\mathbf{p}=p_s(\phi)\mathbf{e}_\phi} = \frac{\alpha p_s(\phi) \mathbf{e}_\phi + \mathbf{B}}{|\alpha p_s(\phi) \mathbf{e}_\phi + \mathbf{B}|}. \quad (\text{S2})$$

Replacing $p_s(\phi)$ by p_F in Eq. (S2), while keeping the density of states on the displaced Fermi surface, produces a spurious anisotropy. This calculation is useful because it isolates the step at which an anisotropic scalar lifetime can enter a relaxation-time treatment.

We use

$$\varepsilon = \frac{m\alpha}{p_F}, \quad \gamma = \frac{B}{\alpha p_F}, \quad \theta = \phi - \phi_B, \quad x_s(\phi) = \frac{p_s(\phi)}{p_F},$$

and

$$l(\theta) = \sqrt{1 + 2\gamma \cos \theta + \gamma^2}.$$

The dimensionless on-shell equation is

$$x_s^2 + 2s\varepsilon\sqrt{x_s^2 + 2\gamma x_s \cos \theta + \gamma^2} = 1, \quad (\text{S3})$$

with the perturbative solution

$$x_s(\theta) = 1 - s\varepsilon\sqrt{1 + 2\gamma \cos \theta + \gamma^2} + \frac{\varepsilon^2}{2}(1 - \gamma^2) + \mathcal{O}(\varepsilon^3). \quad (\text{S4})$$

The angular density of states is written as

$$\rho_s(\phi) = \frac{m}{2\pi} \varrho_s(\phi), \quad \varrho_s(\phi) = \frac{x_s}{x_s + s\varepsilon \boldsymbol{\nu}^{(s)} \cdot \mathbf{e}_\phi}, \quad (\text{S5})$$

where the outer Fermi radius is understood. For this root $v_{s,\parallel} > 0$, so the absolute value in the general radial Jacobian is immaterial.

Using $1/\tau_0 = n_{\text{imp}}|U|^2m$, Eq. (S1) becomes

$$\frac{1}{\tau_s(\phi)} = \frac{1}{\tau_0} \left[\frac{\mathcal{S}}{2} + \frac{s}{2} \boldsymbol{\nu}^{(s)}(\phi) \cdot \mathbf{M} \right], \quad (\text{S6})$$

where

$$\mathcal{S} = \sum_{s'=\pm} \int_0^{2\pi} \frac{d\phi'}{2\pi} \varrho_{s'}(\phi'), \quad \mathbf{M} = \sum_{s'=\pm} s' \int_0^{2\pi} \frac{d\phi'}{2\pi} \varrho_{s'}(\phi') \boldsymbol{\nu}^{(s')}(\phi'). \quad (\text{S7})$$

Thus all branch and angular dependence of the scalar lifetime is contained in the spin-vector spectral weight \mathbf{M} . The scalar spectral weight \mathcal{S} controls only a common, branch-independent part of the rate.

1. Frozen-texture check

We first display the error mode explicitly. Suppose that the angular density of states is evaluated on the true helicity Fermi sheet, but the spin projector is evaluated on the reference contour $p = p_F$. This is not a consistent on-shell projection, but it shows how the apparent anisotropic lifetime is generated.

To the order needed here,

$$\varrho_s(\phi) = 1 - s\varepsilon + \mathcal{O}(\varepsilon\gamma^2, \varepsilon^2). \quad (\text{S8})$$

If the spin texture is frozen on the reference contour $p = p_F$, one uses

$$\boldsymbol{\nu}^{(0)}(\phi) = \frac{\mathbf{e}_\phi + \gamma\mathbf{e}_B}{\sqrt{1 + 2\gamma \cos \theta + \gamma^2}} = \mathbf{e}_\phi + \gamma\mathbf{a}(\phi) + \mathcal{O}(\gamma^2), \quad (\text{S9})$$

with

$$\mathbf{a}(\phi) = \mathbf{e}_B - \cos \theta \mathbf{e}_\phi. \quad (\text{S10})$$

The corresponding spin-vector spectral weight would be

$$\begin{aligned} \mathbf{M}_{\text{fr}} &= \sum_{s=\pm} s \int_0^{2\pi} \frac{d\phi}{2\pi} \varrho_s(\phi) \boldsymbol{\nu}^{(0)}(\phi) = \sum_s s \int_0^{2\pi} \frac{d\phi}{2\pi} (1 - s\varepsilon) (\mathbf{e}_\phi + \gamma\mathbf{a}) + \dots \\ &= -2\varepsilon\gamma \int_0^{2\pi} \frac{d\phi}{2\pi} \mathbf{a}(\phi) + \dots = -\varepsilon\gamma \mathbf{e}_B + \dots, \end{aligned} \quad (\text{S11})$$

where

$$\int_0^{2\pi} \frac{d\phi}{2\pi} \mathbf{a}(\phi) = \frac{1}{2} \mathbf{e}_B. \quad (\text{S12})$$

Substitution into Eq. (S6) would therefore give

$$\frac{1}{\tau_s(\phi)} \Big|_{\text{fr}} = \frac{1}{\tau_0} \left[1 - \frac{s\varepsilon\gamma}{2} \cos(\phi - \phi_B) + \dots \right]. \quad (\text{S13})$$

This is the spurious branch-dependent harmonic produced by the mismatched projection.

The missing term is the on-shell correction to the spin texture. From Eq. (S3), the Fermi-radius displacement is $\delta x_s = -s\varepsilon l + \mathcal{O}(\varepsilon^2)$. One then finds

$$\boldsymbol{\nu}^{(s)}(\phi) = \boldsymbol{\nu}^{(0)}(\phi) + s\varepsilon\gamma \mathbf{a}(\phi) + \mathcal{O}(\varepsilon\gamma^2, \varepsilon^2). \quad (\text{S14})$$

This correction contributes

$$\delta \mathbf{M} = \sum_s s \int_0^{2\pi} \frac{d\phi}{2\pi} s\varepsilon\gamma \mathbf{a}(\phi) + \dots = 2\varepsilon\gamma \int_0^{2\pi} \frac{d\phi}{2\pi} \mathbf{a}(\phi) + \dots = +\varepsilon\gamma \mathbf{e}_B + \dots \quad (\text{S15})$$

Equations (S11) and (S15) cancel. Thus the apparent anisotropic lifetime in Eq. (S13) is not physical; it is removed once the density of states and the spin projector are both evaluated on the same helicity Fermi sheet. The Ward identity in the main text is the nonperturbative version of this cancellation.

2. Consistent on-shell expansion

We now repeat the calculation with the consistent on-shell spin texture. At small γ ,

$$\boldsymbol{\nu}^{(0)}(\phi) = \frac{\mathbf{e}_\phi + \gamma \mathbf{e}_B}{l(\theta)} = \mathbf{e}_\phi + \gamma \mathbf{a}(\phi) + \mathcal{O}(\gamma^2), \quad \mathbf{a}(\phi) = \mathbf{e}_B - \cos\theta \mathbf{e}_\phi. \quad (\text{S16})$$

The branch-dependent displacement of the Fermi sheet changes the spin texture by

$$\delta \boldsymbol{\nu}^{(s)} = s\varepsilon\gamma \mathbf{a}(\phi) + \mathcal{O}(\varepsilon\gamma^2, \varepsilon^2). \quad (\text{S17})$$

Hence

$$\boldsymbol{\nu}^{(s)}(\phi) = \mathbf{e}_\phi + \gamma \mathbf{a}(\phi) + s\varepsilon\gamma \mathbf{a}(\phi) + \mathcal{O}(\gamma^2, \varepsilon\gamma^2, \varepsilon^2). \quad (\text{S18})$$

At the same order,

$$\varrho_s = 1 - s\varepsilon \frac{1 + \gamma \cos\theta}{l(\theta)} + \mathcal{O}(\varepsilon^2) = 1 - s\varepsilon + \mathcal{O}(\varepsilon\gamma^2, \varepsilon^2), \quad (\text{S19})$$

where the term linear in γ cancels in the radial density of states.

Substituting Eqs. (S18) and (S19) into \mathbf{M} gives

$$\begin{aligned} \mathbf{M} &= \sum_s s \int \frac{d\phi}{2\pi} [1 - s\varepsilon] [\mathbf{e}_\phi + \gamma \mathbf{a} + s\varepsilon\gamma \mathbf{a}] + \mathcal{O}(\varepsilon\gamma^2, \varepsilon^2) \\ &= \sum_s \int \frac{d\phi}{2\pi} [s\mathbf{e}_\phi + s\gamma \mathbf{a} + \varepsilon\gamma \mathbf{a} - \varepsilon \mathbf{e}_\phi - \varepsilon\gamma \mathbf{a}] + \mathcal{O}(\varepsilon\gamma^2, \varepsilon^2). \end{aligned} \quad (\text{S20})$$

The two $\varepsilon\gamma \mathbf{a}$ terms cancel before angular integration. The remaining terms vanish either in the branch sum or by $\int (d\phi/2\pi) \mathbf{e}_\phi = 0$. Therefore

$$\mathbf{M} = 0 + \mathcal{O}(\varepsilon\gamma^2, \varepsilon^2). \quad (\text{S21})$$

3. Scalar spectral weight

For completeness, we also check the scalar spectral weight \mathcal{S} to the same order at which it could affect the common part of the rate. The first-order term in Eq. (S19) is odd in the branch index and therefore cancels in the sum over $s = \pm$. Hence

$$\mathcal{S} = 2 + \mathcal{O}(\varepsilon^2). \quad (\text{S22})$$

The ε^2 term can also be evaluated explicitly. Write

$$\boldsymbol{\nu}^{(s)} \cdot \mathbf{e}_\phi = n_0 + s\varepsilon n_1 + \mathcal{O}(\varepsilon^2), \quad n_0 = \frac{1 + \gamma \cos \theta}{l}. \quad (\text{S23})$$

Since

$$\boldsymbol{\nu} \cdot \mathbf{e}_\phi = \frac{x + \gamma \cos \theta}{\sqrt{x^2 + 2\gamma x \cos \theta + \gamma^2}},$$

and $x_s = 1 - s\varepsilon l + \mathcal{O}(\varepsilon^2)$, one obtains

$$n_1 = -\frac{\gamma^2 \sin^2 \theta}{l^2}. \quad (\text{S24})$$

Using Eq. (S3), the denominator of ϱ_s is

$$x_s + s\varepsilon \boldsymbol{\nu}^{(s)} \cdot \mathbf{e}_\phi = 1 + s\varepsilon(n_0 - l) + \varepsilon^2 \left[\frac{1 - \gamma^2}{2} + n_1 \right] + \mathcal{O}(\varepsilon^3), \quad (\text{S25})$$

whereas the numerator is

$$x_s = 1 - s\varepsilon l + \frac{\varepsilon^2}{2}(1 - \gamma^2) + \mathcal{O}(\varepsilon^3). \quad (\text{S26})$$

Expanding the ratio gives

$$\varrho_s = 1 - s\varepsilon n_0 + \varepsilon^2 [n_0(n_0 - l) - n_1] + \mathcal{O}(\varepsilon^3). \quad (\text{S27})$$

The bracket simplifies to

$$n_0(n_0 - l) - n_1 = -\frac{\gamma(1 + \gamma \cos \theta)(\cos \theta + \gamma)}{l^2} + \frac{\gamma^2 \sin^2 \theta}{l^2} = -\gamma \cos \theta. \quad (\text{S28})$$

Therefore

$$\varrho_s(\phi) = 1 - s\varepsilon \frac{1 + \gamma \cos \theta}{l(\theta)} - \varepsilon^2 \gamma \cos \theta + \mathcal{O}(\varepsilon^3). \quad (\text{S29})$$

The first correction is odd in s and cancels in \mathcal{S} . The ε^2 term is independent of s , but its angular average vanishes:

$$\int_0^{2\pi} \frac{d\phi}{2\pi} \cos(\phi - \phi_B) = 0. \quad (\text{S30})$$

Thus

$$\mathcal{S} = 2 + \mathcal{O}(\varepsilon^3) \quad (\text{S31})$$

within the one-contour-per-branch regime.

Equations (S21) and (S31) confirm the mechanism behind the Ward-identity result. The anisotropic term obtained from the density-of-states correction alone is cancelled by the on-shell correction to the spin texture, and the scalar spectral weight gives no field-dependent common correction at the displayed orders. The exact statement, proved in the main text using the Ward identity and the area theorem, is

$$\frac{1}{\tau_s(\phi)} = \frac{1}{\tau_0}. \quad (\text{S32})$$

Thus the perturbative expansion is a consistency check, not an independent source of corrections to the scalar lifetime.

Appendix S3: Weak-field shifted-coordinate proof of the area identity

This section gives an alternative derivation of the two-sheet area identity in coordinates centered at the shifted Rashba degeneracy. In the weak-field regime where the helicity contours are star-shaped with respect to this shifted origin, the cancellation between the two sheets is visible directly in the contour parameterization. The global proof used in the main text is given in Appendix A there.

We align the x -axis with \mathbf{B} and introduce

$$\mathbf{q} = \mathbf{p} + \frac{\mathbf{B}}{\alpha}. \quad (\text{S1})$$

Then

$$|\alpha\mathbf{p} + \mathbf{B}| = \alpha q, \quad (\text{S2})$$

while the kinetic term becomes

$$\frac{p^2}{2m} = \frac{(\mathbf{q} - \mathbf{B}/\alpha)^2}{2m}. \quad (\text{S3})$$

Thus, the energy on helicity sheet $s = \pm$ is

$$\epsilon_s = \frac{(\mathbf{q} - \mathbf{B}/\alpha)^2}{2m} + s\alpha q. \quad (\text{S4})$$

Writing

$$b = \frac{B}{\alpha}, \quad \lambda = m\alpha, \quad R^2 = 2m\mu, \quad (\text{S5})$$

and using polar coordinates around the shifted Rashba point,

$$\mathbf{q} = q(\cos\theta, \sin\theta), \quad (\text{S6})$$

the Fermi-contour equation $\epsilon_s = \mu$ becomes

$$q_s^2 - 2bq_s \cos\theta + b^2 + 2s\lambda q_s = R^2. \quad (\text{S7})$$

For $b < R$, equivalently $\gamma < 1$, the square root below is real for every θ , and the contours are star-shaped with respect to $q = 0$. The positive radial solution is then

$$q_s(\theta) = b \cos\theta - s\lambda + D_s(\theta), \quad (\text{S8})$$

where

$$D_s(\theta) = \sqrt{(b \cos\theta - s\lambda)^2 + R^2 - b^2}. \quad (\text{S9})$$

The occupied area enclosed by sheet s , measured in the same \mathbf{q} -plane, is

$$A_s^{(q)} = \frac{1}{2} \int_0^{2\pi} d\theta q_s^2(\theta), \quad (\text{S10})$$

and the total area is

$$A_{\text{tot}}^{(q)} = A_+^{(q)} + A_-^{(q)} = \frac{1}{2} \sum_{s=\pm} \int_0^{2\pi} d\theta q_s^2(\theta). \quad (\text{S11})$$

We now show that

$$\frac{\partial A_{\text{tot}}^{(q)}}{\partial b} = 0. \quad (\text{S12})$$

Differentiating Eq. (S7) with respect to b at fixed θ , and using

$$q_s + s\lambda - b \cos\theta = D_s, \quad (\text{S13})$$

gives

$$\frac{\partial q_s}{\partial b} = \frac{q_s \cos \theta - b}{D_s}. \quad (\text{S14})$$

Therefore,

$$\frac{\partial A_{\text{tot}}^{(q)}}{\partial b} = \sum_{s=\pm} \int_0^{2\pi} d\theta q_s \frac{q_s \cos \theta - b}{D_s}. \quad (\text{S15})$$

From Eq. (S8),

$$q_s \cos \theta - b = (b \cos \theta - s\lambda + D_s) \cos \theta - b = D_s \cos \theta - b \sin^2 \theta - s\lambda \cos \theta. \quad (\text{S16})$$

Thus, the contribution of branch s to Eq. (S15) can be written as

$$I_s^{(q)} \equiv \int_0^{2\pi} d\theta q_s \frac{q_s \cos \theta - b}{D_s} = \int_0^{2\pi} d\theta \left[q_s \cos \theta - \frac{q_s}{D_s} (b \sin^2 \theta + s\lambda \cos \theta) \right]. \quad (\text{S17})$$

Using

$$\frac{q_s}{D_s} = 1 + \frac{b \cos \theta - s\lambda}{D_s}, \quad (\text{S18})$$

we split this as

$$I_s^{(q)} = \int_0^{2\pi} d\theta [q_s \cos \theta - b \sin^2 \theta - s\lambda \cos \theta] - \int_0^{2\pi} d\theta \frac{(b \sin^2 \theta + s\lambda \cos \theta) (b \cos \theta - s\lambda)}{D_s}. \quad (\text{S19})$$

Consider first the nonsingular part. Substituting $q_s = b \cos \theta - s\lambda + D_s$, we find

$$\sum_s \int_0^{2\pi} d\theta [q_s \cos \theta - b \sin^2 \theta - s\lambda \cos \theta] = \sum_s \int_0^{2\pi} d\theta [b(\cos^2 \theta - \sin^2 \theta) + D_s \cos \theta - 2s\lambda \cos \theta]. \quad (\text{S20})$$

The first and last terms integrate to zero over a full period. The remaining term cancels between the two helicity branches because

$$D_-(\theta) = D_+(\theta + \pi), \quad \cos(\theta + \pi) = -\cos \theta. \quad (\text{S21})$$

Hence,

$$\sum_s \int_0^{2\pi} d\theta D_s(\theta) \cos \theta = 0. \quad (\text{S22})$$

The second term in Eq. (S19) contains the numerator

$$(b \sin^2 \theta + s\lambda \cos \theta) (b \cos \theta - s\lambda) = b^2 \sin^2 \theta \cos \theta + bs\lambda \cos 2\theta - \lambda^2 \cos \theta. \quad (\text{S23})$$

Therefore,

$$\frac{\partial A_{\text{tot}}^{(q)}}{\partial b} = - \sum_s \int_0^{2\pi} d\theta \frac{b^2 \sin^2 \theta \cos \theta + bs\lambda \cos 2\theta - \lambda^2 \cos \theta}{D_s(\theta)}. \quad (\text{S24})$$

Under $\theta \rightarrow \theta + \pi$, one has $D_-(\theta) = D_+(\theta + \pi)$. The terms proportional to $\sin^2 \theta \cos \theta$ and $\cos \theta$ change sign and cancel between $s = +$ and $s = -$. The term proportional to $s \cos 2\theta$ has a π -periodic numerator, so the two denominator-mapped integrals are equal, while the explicit factor s makes them cancel. Thus, Eq. (S24) vanishes.

Combining the two parts gives

$$\frac{\partial A_{\text{tot}}^{(q)}}{\partial b} = 0, \quad \gamma < 1. \quad (\text{S25})$$

This proves the area identity in the regime where the shifted-coordinate polar representation is globally valid.

The shifted-coordinate derivation is the weak-field local form of the global area identity proved in Appendix A of the main text. The latter uses the original momentum coordinate and applies throughout the continuum two-sheet regime used for the main conductivity calculation.